RESEARCH ARTICLE OPEN ACCESS

Glycine Receptor β–Targeting Autoantibodies Contribute to the Pathology of Autoimmune Diseases

Anna-Lena Wiessler, MSc, Ivan Talucci, MSc, Inken Piro, MSc, Sabine Seefried, MSc, Verena Hörlin, Betül B. Baykan, MD, Erdem Tüzün, MD, Natascha Schaefer, Dr., Hans M. Maric, Dr., Claudia Sommer, MD, and Carmen Villmann, Prof. Dr.

Correspondence
Dr. Villmann
villmann_c@ukw.de

Neurol Neuroimmunol Neuroinflamm 2024;11:e200187. doi:10.1212/NXI.0000000000200187

Abstract

Background and Objectives

Stiff-person syndrome (SPS) and progressive encephalomyelitis with rigidity and myoclonus (PERM) are rare neurologic disorders of the CNS. Until now, exclusive GlyRα subunit–binding autoantibodies with subsequent changes in function and surface numbers were reported. GlyR autoantibodies have also been described in patients with focal epilepsy. Autoimmune reactivity against the GlyRβ subunits has not yet been shown. Autoantibodies against GlyRα1 target the large extracellular N-terminal domain. This domain shares a high degree of sequence homology with GlyRβ making it not unlikely that GlyRβ-specific autoantibody (aAb) exist and contribute to the disease pathology.

Methods

In this study, we investigated serum samples from 58 patients for aAb specifically detecting GlyRβ. Studies in microarray format, cell-based assays, and primary spinal cord neurons and spinal cord tissue immunohistochemistry were performed to determine specific GlyRβ binding and define aAb binding to distinct protein regions. Preadsorption approaches of aAbs using living cells and the purified extracellular receptor domain were further used. Finally, functional consequences for inhibitory neurotransmission upon GlyRβ aAb binding were resolved by whole-cell patch-clamp recordings.

Results

Among 58 samples investigated, cell-based assays, tissue analysis, and preadsorption approaches revealed 2 patients with high specificity for GlyRβ aAb. Quantitative protein cluster analysis demonstrated aAb binding to synaptic GlyRβ colocalized with the scaffold protein gephyrin independent of the presence of GlyRα1. At the functional level, binding of GlyRβ aAb from both patients to its target impair glycine efficacy.

Discussion

Our study establishes GlyRβ as novel target of aAb in patients with SPS/PERM. In contrast to exclusively GlyRα1-positive sera, which alter glycine potency, aAbs against GlyRβ impair receptor efficacy for the neurotransmitter glycine. Imaging and functional analyses showed that GlyRβ aAbs antagonize inhibitory neurotransmission by affecting receptor function rather than localization.

MORE ONLINE

Graphical Abstract
links.lww.com/NXI/A971

From the Institute for Clinical Neurobiology (A.-L.W., V.H., N.S., C.V.), University of Wuerzburg; Department of Neurology (I.T., I.P., S.S., C.S.), University Hospital Wuerzburg; Rudolf Virchow Center for Integrative and Translational Bioimaging (I.T., H.M.M.), University of Wuerzburg, Germany; Department of Neurology (B.B.B.), Istanbul Faculty of Medicine; and Institute of Experimental Medical Research (E.T.), Istanbul University, Turkey.

Go to Neurology.org/NN for full disclosures. Funding information is provided at the end of the article.

The Article Processing Charge was funded by the authors.

Glossary

aAb = autoantibody; **GlyR** = glycine receptor; **Pat** = patient; **PERM** = progressive encephalitis with rigidity and myoclonus; **SPS** = stiff-person syndrome.

Introduction

Stiff-person syndrome (SPS) is a rare autoimmune disease of the CNS with a prevalence of 1:1.000.000. Severe cases of SPS are associated with progressive encephalitis with rigidity and myoclonus (PERM).[1] Most common symptoms include muscle spasms, stiffness of abdominal and limb muscles, exaggerated startle, and different forms of phobias.[2,3]

So far, glycine receptor (GlyR) autoantibody (aAb) have been found to bind GlyRα subunits expressed in spinal cord neurons and tissue without subtype preferences.[4] Epitope characterization identified a common N-terminal region in the GlyRα1 subunit with residues A^{29}-G^{62} for aAb binding.[5] GlyR aAbs are able to cross-link receptors followed by subsequent internalization.[4] Moreover, GlyR aAb binding impairs receptor function by direct blocking of most likely structural transitions essential for ion channel opening.[5,6]

There are 4 GlyR α subunits (α1-4) and one β subunit with each subunit consisting of a large extracellular domain (ECD), 4 transmembrane domains (TM1-4) connected by loop structures, and a short extracellular C-terminus.[7-9] These subunits form pentameric chloride channels composed of α-homomers or αβ-heteromers.[10,11] While GlyR homomers have been found at presynaptic sites involved in the control of glycine release[12] and at extrasynaptic sites at postsynapses, GlyR heteromers form the synaptically localized receptors in postsynaptic neurons. The GlyRβ subunit in heteromeric GlyRs is essential because it harbors the binding site for the scaffold protein gephyrin, which stabilizes GlyR complexes at postsynaptic sites.[13] A constant packing of 2,000 GlyRs μm^{-2} at spinal cord synapses throughout adulthood has been estimated.[14]

Besides its structural role, GlyRβ also contributes to GlyR function.[15] Genetic human and murine variants of GlyRβ associated with startle disease, which share phenotypic symptoms with SPS, have been determined with functional impairments of glycine potency and efficacy accompanied by less synaptic localization.[16-18]

In this study, we identified 2 patients with aAbs not only binding GlyRα but also the GlyRβ subunit. Using patient serum samples, we investigated whether and how the disease pathology of GlyRβ SPS differs from GlyRα SPS at the molecular, cellular, and functional levels.

Methods

Patients

Fifty-eight patient serum samples were submitted to our laboratory. In 48 patients, SPS was suspected, and they were negative for antiglutamate-decarboxylase and antiamphiphysin aAb. In 10 patients, a focal epilepsy of unknown cause was present, and GlyR aAb were found by routine screening. None of the patients with epilepsy had motor symptoms, hyperekplexia, or startle reaction.[19] Disease pattern of 2 patients with GlyRαβ aAb (Pat31 and Pat36) in comparison with 1 patient with GlyRα aAb only (Pat11) are further described in the Table.

Ethical Statement

Experiments using patient material have been approved by the Ethics Committee of the Medical Faculty, University of Würzburg, Germany ("Glycine receptor autoantibodies and spinal disinhibition," 20190424 01).

Anxiety Questionnaires

Patients underwent a neurologic examination, and Pat11 and Pat36 were given questionnaires about chronic pain,[20,21] anxiety (Liebowitz Social Anxiety Scale [LSAS]; Anxiety Sensitivity Index [ASI]),[22,23] and heightened sensitivity inducing spasms and falls (see Table for results).[24]

Cell Lines

HEK-293 cells (Human Embryonic Kidney cells; CRL-1573; ATCC—Global Bioresource Center) were used for in vitro experiments. Cells were grown in minimum essential medium (Life Technologies, Carlsbad, US) supplemented with 10% fetal bovine serum, L-glutamine (200 mM), and 100 U/mL penicillin and 100 μg/mL streptomycin at 37°C and 5% CO_2.

Primary Spinal Cord Neurons

Neurons were prepared from embryos of a novel generated hybrid mouse line *Glra1*^{spdot}/*Glrb*^{eos} from *Glrb*^{eos14} and *Glra1*^{spdot} (*oscillator*, JAX stock #000536, JAX:000536, Jackson Laboratory, Bar Harbor, US) at the embryonic stage 12–13. Experiments were approved by the local veterinary authority (Veterinäramt der Stadt Würzburg, Germany) and the Ethics Committee of Animal Experiments, i.e., Regierung von Unterfranken, Würzburg, Germany (license no.:55.2.2-2532.2-949-31). Mixed spinal cord neuronal cultures were prepared as previously described.[25] Genotyping for *Glrb*^{eos} and *Glra1*^{spdot} was performed according to Maynard et al.[14] Stainings and electrophysiologic measurements were performed after 16–18 days in culture.

Transfection of Cells

HEK-293 cells were transiently transfected by using a modified calcium phosphate precipitation method.[18]

Immunocytochemistry

Living transfected HEK-293 cells or primary neurons were incubated for 2 hours at 4°C with patient sera, healthy control serum (1:50), or commercial antibody against GlyRα1

Table Patient Characteristics

	Patient 31: alpha & beta	Patient 36: alpha & beta	Patient 11: alpha
Sex	Male	Male	Male
Age at blood withdrawal	58 y	68 y	44 y
Disease duration	48 y	16 y	19 y
Diagnosis	Focal epilepsy	SPS/PERM	SPS
Symptom history	Focal epilepsy with restless legs syndrome, insomnia, diabetes mellitus, chronic renal failure	Brainstem myoclonus and exaggerated startle response sensitive to minor auditory and tactile stimuli, abnormal eye movements with diplopia and nystagmus	Recurrent lockjaw associated with limb stiffness, startle, and frequent falls
Tested negative for other aAbs	NMDAR, LGI1, Caspr2, $GABA_AR$, AMPAR, GAD	NMDAR, LGI1, Caspr2, $GABA_AR$, AMPAR, GAD	NMDAR, LGI1, Caspr2, $GABA_AR$, AMPAR, GAD
Current symptoms	Intact	Under current medication, no increased muscle tone, no paresis, normal gait	Under current medication, reduced frequency of symptoms
Medication	Carbamazepine 600 mg pramipexole 0.75 mg	Steroid pulse therapy at 4-wk intervals with 4 ×1,000 mg methylprednisolone Clonazepam 2.5 mg Pramipexol 2 mg levodopa/benserazid 100/25 mg as needed	Clonazepam 8 mg 1-1-1 Δ^9-Tetrahydrocannabinol/cannabidiol (Sativex spray) as needed Immunoadsorption every 4 wk
Pain (graded chronic pain scale, scale 0–4)	0	0	3
Anxiety sensitivity index, scale 0–72)	n.d.	29	38
Social anxiety and avoidance	Moderate to severe	Very mild	Very mild
Scale of increased sensitivity[a], 0–7)		3, noise, somatosensory and emotional excitement	4, noise and visual, somatosensory, and emotional excitement

Abbreviation: PERM = progressive encephalomyelitis with rigidity and myoclonus; SPS = stiff-person syndrome.
[a] Dalakas et al. 2017.[43].

(146111, 1:500, Synaptic Systems, Göttingen, Germany). After fixation using 4% paraformaldehyde/4% sucrose in phosphate-buffered saline (PBS) at pH 7.4 for 20 minutes at room temperature (RT), cells were blocked and permeabilized with 5% goat serum/0.2% Triton-X-100 in PBS for 30 minutes. Primary antibodies against myc-tagged GlyRβ (303008, 1:250, Synaptic Systems), gephyrin (147111, 1:500, Synaptic Systems), synapsin (574778, 1:500, Merck), and pan-α-GlyR (146011, 1:250, Synaptic Systems) were incubated for 1 hour, followed by incubation with secondary antibodies (all 1:500, 111-546-003, 109-165-003, 115-175-146, and 111-175-006, all from Dianova, Hamburg, Germany) for 1 hour. Cell nuclei were stained with 4′,6-diamidino-2-phenylindole (DAPI) and mounted in Mowiol.

Preadsorption

Living HEK-293 cells transfected with the GlyRα1 subunit were incubated with patient sera, healthy control serum (1:50), or GlyRα1 antibody (146111, 1:500, Synaptic Systems) for 1 hour at RT. The supernatant containing unbound antibodies was transferred to another coverslip with 3 repetitions. Finally, the supernatant was transferred to HEK-293 cells transfected with the zebrafish GlyRα1 and human GlyRβ subunit.

ELISA Neutralization With GlyRα1 ECD

GlyRα1 ECD preparation and enzyme-linked immunosorbent assay (ELISA) were performed as described previously.[26] Spinal cord neurons were stained afterward with patient serum (1:50).

Immunohistochemistry

Spinal cords were extracted from anesthetized $Glra1^{+/+}/Glrb^{eos/eos}$ and $Glra1^{spdot/spdot}/Glrb^{eos/eos}$ mice, bedded in Tissue-Tek and immediately frozen on dry ice. A cryostat (CM1950, Leica, Wetzlar, Germany) with a chamber temperature of −20°C was used to cut spinal cord sections of 9 µm thickness. Sections were mounted on SuperFrost Plus slides (03-0060, Langenbrinck, Niederrohrdorf, Switzerland).

Sections were fixed with ice-cold 2% paraformaldehyde in PBS at pH 7.4 for 30 seconds at RT. After washing, sections

were shortly dipped in 50 mM NH_4Cl for quenching and incubated in 0.1 mM glycine for 30 minutes. For blocking, 10% goat serum in PBS at pH 7.4 was used followed by primary antibody incubation with patient serum (1:50) and an anti–mEos-Cy3 (N3102-SC3-L, 1:200, Nanotag, Göttingen, Germany) overnight (ON) at 4°C. Secondary antibody goat-anti-human-IgG-Alexa-Fluor-647 (1:500, JIM-109-605-006, Biozol, Eching, Germany) was incubated for 1 hour at RT. Nuclei were stained with DAPI for another 10 minutes. Sections were covered with Fluor Save Reagent (345789, Calbiochem, Darmstadt, Germany).

Pentameric Structure of GlyR

The cryo-EM structure (7MLY[9]) of the pentameric GlyR with a subunit stoichiometry of 4α:1β was used to generate structural images. Figures were prepared with the help of Pymol (pymol.org, version 2.0.7).

µSPOT Synthesis

GlyR subunit ECDs (UniProtKB: P23415, P23416, O75311, Q5JXX5, P48167) were displayed in microarray format as 15mer overlapping peptide library. µSPOT[27] peptide microarrays were synthesized using a MultiPep RSi robot (CEM, Matthews, US) on cellulose discs containing 9-fluorenylmethyloxycarbonyl-β-alanine (Fmoc-β-Ala) linkers (average loading: 130 nmol/disc—4mm diameter). Synthesis was performed by deprotecting the Fmoc-group using 20% piperidine in dimethylformamide (DMF). Peptide chains were elongated using a coupling solution consisting of amino acids (0.5 M) with oxyma (1 M) and diisopropylmethanediimine (1 M) in DMF (1:1:1). Coupling steps were conducted 3 times (30 minutes), followed by capping (4% acetic anhydride in DMF). Side chains were deprotected using 90% trifluoracetic acid (TFA), 2% dichloromethane (DCM), 5% H_2O, and 3% triisopropylsilane (TIPS, 150 µL/well) for 1 hour at RT. Afterward, the deprotection solution was removed, and the discs were solubilized ON at RT using a solvation mixture containing 88.5% TFA, 4% trifluoromethanesulfonic acid, 5% H_2O, and 2.5% TIPS. The resulting peptide-cellulose conjugates (PCCs) were precipitated with ice-cold ether and spun down at 2,000×*g* for 10 minutes at 4°C, followed by 2 additional washes with ice-cold ether. Resulting pellets were dissolved in DMSO. PCC solutions were mixed 2:1 with saline–sodium citrate buffer (150 mM NaCl, 15 mM trisodium citrate, pH 7.0) and transferred to a 384-well plate. For transfer of the PCC solutions to white-coated CelluSpot blank slides (76 × 26 mm, Intavis AG Peptide Services, Tübingen, Germany), a SlideSpotter was used.

Microarray Binding Assay

Microarray slides were blocked for 1 hour in 5% (w/v) milk powder, 0.05% Tween20, and PBS at pH 7.4. The slides were incubated for 30 minutes with positive and negative sera (1:500) or GlyRα1 and GlyR pan-α antibody (1:2500) in blocking buffer. IgG antibodies were detected using goat-anti-human or goat-anti-mouse-IgG-HRP (31410, 1:2500, 31430, 1:5000, Thermo Fisher, Waltham, US). The readout was detected with an Azure imaging system c400 using Super-Signal West Femto substrate (Thermo Scientific). Microarray binding intensities were quantified with FIJI using the "microarray profile" plugin (OptiNav Inc, Bellevue, US).

Neutralization in Microarray Format

Cleavable peptides were synthesized with an additional rink amide linker at the C-terminus of the identified epitope. Microarray slides were blocked using 5% (w/v) milk powder, 0.05% Tween20, and PBS at pH 7.4 for 1 hour. Serum samples from patient 36 were preincubated with cleaved peptide in the amount corresponding to 2 and 4 cellulose discs containing Fmoc-β-Ala linkers. Peptides were resuspended in 100 µL of PBS buffer, and 5 µL of serum was added subsequently. The samples were mixed at 1000 rpm (RT) for at least 30 minutes. A control without peptide was treated in the same manner. Solutions were added to 2.5 mL of blocking solution and incubated for 30 minutes on the slides. Microarray binding intensities were quantified with FIJI and normalized against the untreated slide.

Electrophysiologic Recordings

Patch-clamp analysis was performed on transfected HEK-293 cells or mixed primary neuronal cultures using whole-cell recordings. Experiments were performed at 21°C. Recording pipettes were pulled from borosilicate capillaries with open resistances of 3.5–5.5 MΩ and filled with internal buffer in mM (120 CsCl, 20 $N(Et)_4Cl$, 1 $CaCl_2$, 2 $MgCl_2$, 11 EGTA, 10 HEPES for HEK-293 cells; 140 CsCl, 1 EGTA, 10 HEPES, and 6 D-Glucose for neurons; pH 7.2, adjusted with CsOH). For determination of maximal current amplitudes (I_{max}) and dose-response curves (EC_{50} values), glycine was applied in a concentration series of 10–1000 µM in external buffer in mM (137 NaCl, 5.4 KCl, 1.8 $CaCl_2$, 1 $MgCl_2$, 5 HEPES for HEK-293; 130 NaCl, 3 KCl, 1.5 $CaCl_2$, 2 $MgCl_2$, 10 HEPES, 6 D-Glucose, and 10 TEA-Cl for neurons; pH 7.35, adjusted with NaOH). Glycine solutions were applied by the Octaflow II system (ALA Scientific Instruments, Farmingdale, US). Following recordings, 50 µM picrotoxinin (Sigma Aldrich, Darmstadt, Germany) + 100 µM glycine were applied. Homomeric GlyRα, but not heteromeric GlyRαβ, are blocked by picrotoxinin.[28] This test was used to discriminate between homomeric and heteromeric receptors. Current responses were amplified with an EPC-10 amplifier and measured at a holding potential of −60 mV using Patchmaster Next software (HEKA Elektronik, Reutlingen, Germany).

Western Blot Analysis

Spinal cord, brainstem, and cortex samples were extracted from deeply anesthetized male and female mice and directly frozen at −80°C. Lysate were prepared using 1 mL of brain homogenisate buffer (20 mM HEPES, 100 mM potassium acetate, 40 mM KCl, 5 mM EGTA, 5 mM $MgCl_2$, 5 mM DTT, 1% TritonX-100, 1 mM PMSF, and protease inhibitors (Roche, Basel, Switzerland). After a 15-minute centrifugation at 10.000×*g* at 4°C, supernatants were transferred and used for Western blots.

Protein samples were separated by SDS-PAGE using 11% (w/v) gels followed by transfer of proteins onto a nitrocellulose membrane (GE Healthcare, München, Germany). After blocking for 1 hour with 5% BSA in TBS-T (TBS with 1% v/v Tween20), membranes were incubated with primary antibodies anti-gephyrin, anti-GlyR pan-α, anti-GlyRα1, anti-VGAT (131003) all 1:1,000, Synaptic Systems), and anti-GAPDH (CB1001, 1:1,000, Merck) ON at 4°C. Proteins were visualized by horseradish peroxidase–coupled secondary antibodies (111-036-003 and 115-035-146, 1:15000, Dianova) and detected through chemiluminescence using clarity Western ECL substrate (170-5061, BioRad, Feldkirchen, Germany).

Experimental Design and Statistical Analysis

Images were captured using an Olympus Fluoview ix1000 microscope (UPLSAPO 60× oil objective) or a Zeiss Axio Imager 2 microscope (20× air objective). For image analysis and processing, the Fiji/ImageJ software was used.[29] Synaptic density/100 μm was analyzed through the plug-ins NeuronJ and SynapscountJ.

Data were analyzed using GraphPad Prism or Origin9 software and represented as mean ± standard error of the mean (SEM).

The numbers of experiments (N; all experiments have been performed from 3 biological replicates or as stated otherwise) and cells (n) are listed in eTable 1 (links.lww.com/NXI/A969). Data were tested for outliers by ROUT (Q = 1%). Normality of the data was reviewed by the Shapiro-Wilk normality test ($\alpha = 0.05$). Statistical significance was calculated using an unpaired 2-tailed Mann-Whitney test or an unpaired t test. p values are given in the result section or eTable 1. The 0-hypothesis was rejected at a level of $p < 0.05$.

Data Availability

Data that support the findings of this study are available from the corresponding author on reasonable request.

Results

The GlyRβ Subunit Represents a Target for GlyR aAb

GlyR aAb have been identified to target a common sequence in the ECD of GlyRα subunits (Figure 1A).[5] The adult receptor composition is 4α:1β heteromeric.[8,9] The GlyRα ECD shares a high homology to the GlyRβ subunit (Figure 1B). In this study, we investigated 58 serum samples from patients with SPS-like symptoms and focal epilepsy and tested them for binding to GlyRβ (Figures 1A and 2, A–D). GlyRβ subunit alone does not form functional channels[8,9,30] and requires coexpressed α for transport to the plasma membrane (Figure 2B). Thirty samples harbored aAb against human GlyRα1 (eFigure 1A, links.lww.com/NXI/A966), whereas 28 displayed no binding. All GlyRα1-negative sera demonstrated also no binding to human GlyRβ subunits (selected examples; eFigure 1B, eTable 2, links.lww.com/NXI/A970).

To analyze whether GlyRα1-positive sera bind GlyRβ, we used zebrafish GlyRα1^{dr} to ensure transport and integration of GlyRβ into the cellular membrane (Figure 2B). Previously, we have shown that most human serum samples harboring GlyRα aAb do not bind zebrafish α1.[5] Three patient sera of the 30 GlyRα1-positive sera bound to the zebrafish α1 subunit and were thus excluded from further analysis. Testing of the remaining 27 human GlyRα1-positive sera resulted in GlyRβ binding of Pat 31 and Pat 36 suggesting that indeed GlyRβ represents a target for GlyR aAb (Figure 2D, eTable 2, links.lww.com/NXI/A970). Both patients had a confirmed autoimmune disorder. Pat31 had focal epilepsy without any other cause than GlyR aAb, and Pat36 had unequivocal SPS/PERM with good response to immunotherapy (Table). Detailed information is published elsewhere (Pat11,[31] Pat31,[19,32,33] and Pat36[26]).

Single-nucleotide variations in the GlyRβ subunit gene have been associated with an increased susceptibility to anxiety or panic disorders identified in a genome-wide association study with healthy human volunteers.[34,35] However, anxiety scores of patients with GlyRβ aAb (Pat31, Pat36) were not different from Pat11 with exclusively GlyRα aAb (Table).

Identification and Mapping of GlyRβ Subunit aAb Epitopes

Peptide microarray-based screenings enable the identification, mapping, and validation of linear aAb epitopes (Figure 3A).[36] To identify possible binding regions of GlyRβ aAb, GlyR subunits α1-4 and β were displayed in form of 372 peptides (15 amino acids (AA) length, 10AA overlap, 5AA shift). The recapitulation of the reported epitopes of commonly used GlyR antibodies mAb2b and mAb4a confirms the microarray capacity to report binding epitopes within the structured GlyR ECD (Figure 3, B–D). The same arrays reported putative aAb binding sites for Pat31 and Pat36, which confirmed binding to the GlyRβ subunit. Pat31 showed reactivity toward GlyRα1/α4/β subunits, whereas Pat36 showed pan-GlyR subunit activity (Figure 3, B and C). A focused GlyRβ library of 232 peptides (15AA length, 14AA overlap, 1AA shift) determined GlyRβ sequences that may mediate aAb binding. An autoantibody epitope for Pat36 was mapped toward GlyRβ residues ^{141}PDLFFANEKSANFHDV^{156} and for Pat31 toward ^{77}GIPVDVVVNIFINSF^{91} (Figure 3D). The observation that GlyRβ aAb binding of Pat 36 partially overlaps with the epitope of mAb4a suggests an elevated intrinsic immunogenic potential of this region. Both identified GlyRβ epitopes are localized within surface-accessible GlyRβ ECD β sheets (Figure 3, E and F).

To confirm the microarray mapping and to verify the observed anti-GlyRβ reactivity, we conducted on-chip neutralization experiments. In this study, serum of Pat36 was preincubated with increasing amounts of the soluble GlyR peptide (DSIWKPDLFFANEKG) that overlaps with the mapped binding site. The observed concentration-dependent signal reduction upon preadsorption (Figure 3G) supports the conclusion that the microarray binding signals resulted from sequence-specific GlyRβ recognition of the patient aAb.

Figure 1 Overview of Reported GlyR Antibody and Autoantibody Epitopes

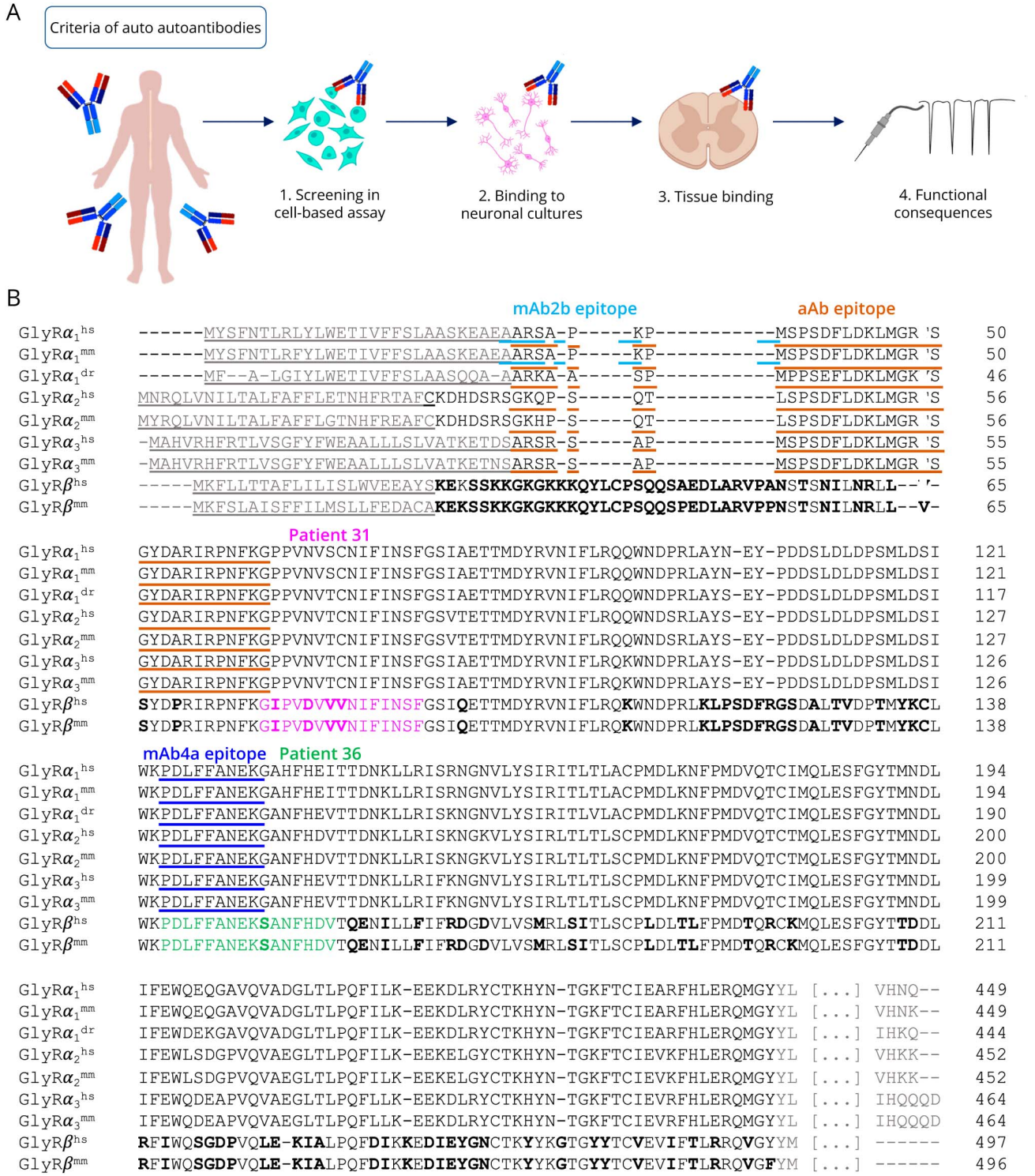

(A) Determination of autoantibody specificity by cell-based assays and neuronal and tissue binding and functional analysis in the presence of aAbs. (B) Alignment of GlyR subunits α1, α2, α3 and β from human and mouse and α1 from zebrafish concentrating on the ECD. Numbers of amino acids refer to nonmature protein. Labeled are the binding epitopes of the commercial GlyRα1 (mab2b) (cyan) and pan-α (mab4a) (blue) antibodies. In addition, the aAb epitope ^{29}A-^{62}G for GlyRα aAb binding is marked (brown).[5] The here mapped sequences for aAb binding (green and magenta) are marked. Numbers of amino acids refer to nonmature protein.

Figure 2 Screening of Patient Samples Identifies Anti-GlyRβ aAb

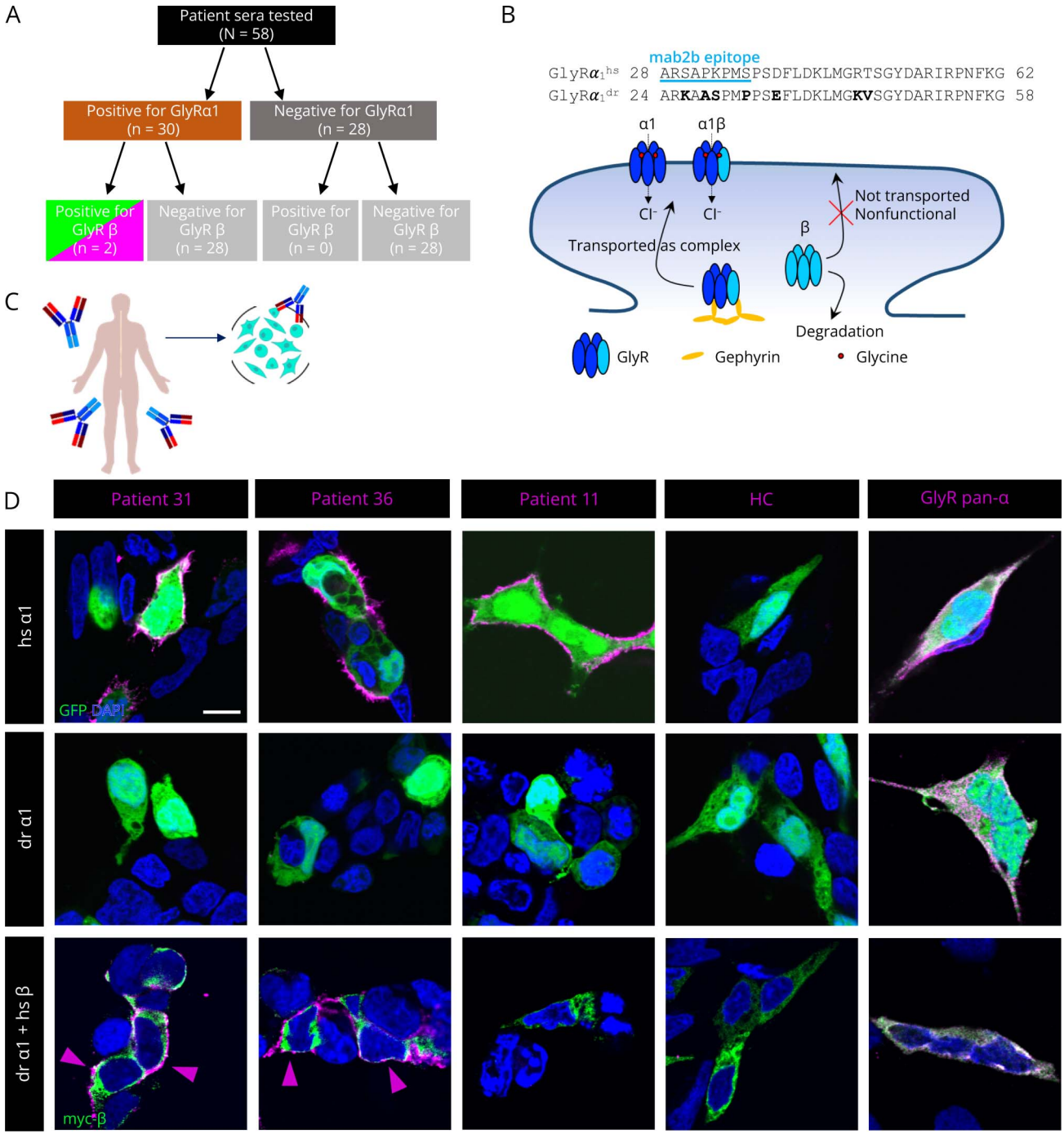

(A) Flowchart for the screening of sera from patients with SPS-like symptoms. Of 58 patient sera, 30 samples were positive for GlyRα1 aAb of which 2 were also positive for the GlyRβ subunit. All patient serum samples negative for GlyRα1 aAb were also negative for binding to GlyRβ. (B) Alignment of the postulated aAb epitope of human (hs) and zebrafish (dr) GlyRα. Scheme of the GlyR complex transport to the plasma membrane. GlyRβ alone cannot form function ion channels and therefore is not transported to the membrane but degraded. (C) Principle of cell-based assay. (D) Binding of serum samples of Pat31, Pat36, Pat11, healthy control (HC) serum, and a commercial antibody against the GlyRα subunits to transfected HEK-293 cells. Cells were cotransfected either with GFP (green) and different GlyRα subunits from human (hs) and zebrafish (dr) or with zebrafish GlyRα1 and a myc-tagged human GlyRβ. GlyRβ is stained with an antimyc antibody (green, lower panel), binding of patient serum was verified with an anti-human-IgG-Cy3 antibody (magenta), and expression control of GlyRα is also demonstrated (magenta, right panel). Arrows point to binding of patient serum to transfected HEK-293 cells. Note, the detection of the GlyRβ subunit through the myc antibody required cell fixation and permeabilization, leading to surface membrane and intracellular staining of GlyRβ. Scale bar refers to 10 μm.

Figure 3 Epitope Mapping of GlyRβ aAbs Through Peptide Microarrays

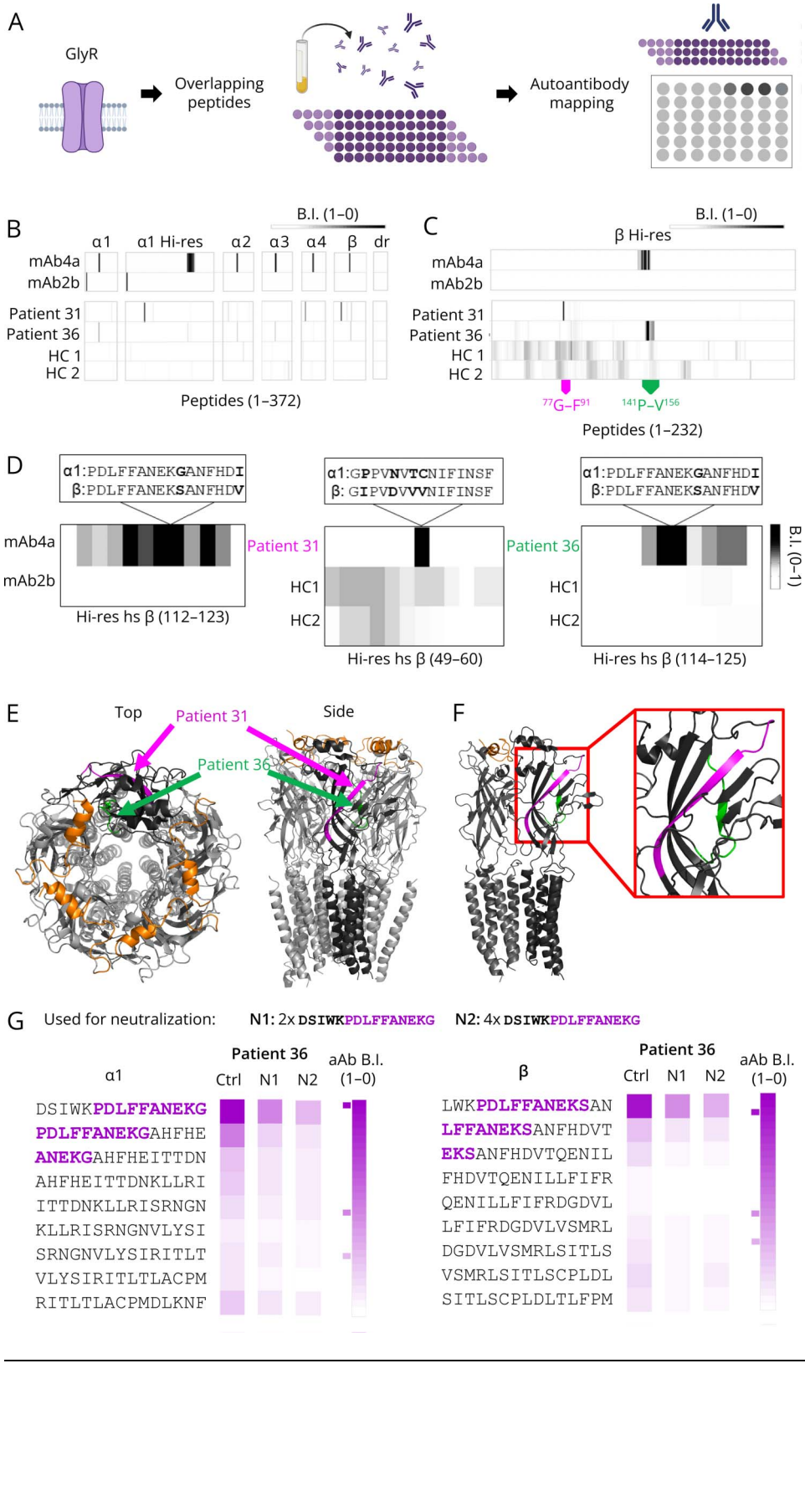

(A) Array workflow. GlyRα1-4 and β sequences were extracted from Uniprot. From those sequences, overlapping peptide libraries were synthetized in μSPOT format. Peptide microarrays were incubated with serum samples from antiglycine receptor–positive patients. Epitope binding sequences were detected by chemiluminescence. (B) Shown are normalized heatmap binding intensities for Pat31 and Pat36, HC, and glycine receptor monoclonal antibodies incubated on the microarrays with all the different subunits displayed (α1-4 and β). Each line corresponds to a peptide signal on the microarray. Pat31 shows binding on the α1, α4, and β subunits, whereas Pat36 shows pan-activity similarly to the mAb4a. (C–D) Detailed heatmap within the region of GlyRβ binding by the pan-GlyR antibody mAb4a, and patients (Pat31, Pat36). (E) Crystal structure of the human GlyR heteropentamer (PDB: 7MLY)[9] as top and side view with aAb epitopes marked (GlyRα orange, GlyRβ magenta and green). (F) Right image shows GlyRα-β dimer interface. (G) Each GlyR subunit was displayed as overlapping peptides with 5 amino acids shift. Sera were probed without peptide (Ctrl) or by using increasing cleavable peptide amounts (N1 and N2—purple shades—correspond to the peptide amounts of 2–4 cellulose-cleavable discs that were preincubated with serum 36). Autoantibody binding was depicted as heatmap by normalizing detected intensities against the non-neutralized sera, where 1 corresponds to the α1 signal for DSIWKPDLFFANEKG sequence.

Specific GlyRβ aAbs Are Not Preabsorbed by GlyRα1

To confirm specific GlyRβ binding of patient sera, GlyRα1 expressed in transfected HEK-293 cells were used for preadsorption of GlyRα1-specific aAbs from patient serum. As a second approach, incubation of patient serum with the purified and refolded GlyRα1 ECD coated to ELISA plates was used.[26] We transferred patient serum 3 times to transfected HEK-293 cells expressing only GlyRα1 for 1 hour followed by live staining of the remaining supernatant on HEK-293 cells expressing GlyRα1 and GlyRβ. As control, we used an exclusively GlyRα1-positive serum with the same titer as Pat31 and Pat36 for better comparison (titer 1:500).

Serum signals of Pat31 and Pat36 were already strongly reduced after the first transfer and completely abolished after the second one, whereas binding of Pat12 serum was no longer visible after 3 transfers (Figure 4A). Final transfer of the samples to GlyRα1 and GlyRβ expressing cells revealed again binding of Pat31 and Pat36 sera but not binding of Pat12 serum arguing that GlyRβ-specific aAbs still remained in the serum.

Then patient samples were incubated with the ECD of GlyRα1 bound to ELISA plates, and the remaining supernatant was used for live staining of spinal cord neurons (Figure 4B). Although Pat36 and Pat12 sera both bound very strongly to spinal cord neurons before the adsorption by GlyRα1 ECD, remaining signal was only detectable for Pat36 serum afterward. Together, these findings further confirm that both, Pat31 and Pat36, sera contain aAb targeting GlyRβ and cannot be neutralized by GlyRα1. Due to insufficient material from Pat31, this and some following experiments were performed only with Pat36 serum.

GlyRβ aAbs Bind Specifically to Endogenous β Subunits

The binding of GlyRβ-positive patient sera to endogenous GlyRs was evaluated using murine mixed spinal cord cultures isolated from a mouse model that allows specifically the detection of GlyRβ. *Glra1*$^{spdot/spdot}$/*Glrb*$^{eos/eos}$ animals result from crossing mEos4-tagged *Glrb*[14] with *Glra1* mutant *oscillator* mice.[37] *Oscillator* mice carry a frameshift mutation resulting in lack of GlyRα1 in homozygous animals. Binding of Pat31 and Pat36 sera were detected in both *Glra1*$^{+/+}$/*Glrb*$^{eos/eos}$ (wild-type controls) and *Glra1*$^{spdot/spdot}$/*Glrb*$^{eos/eos}$ neurons (absence of GlyRα1). Pat12 serum bound to *Glra1*$^{+/+}$/*Glrb*$^{eos/eos}$ but not *Glra1*$^{spdot/spdot}$/*Glrb*$^{eos/eos}$ neurons lacking GlyRα1 (Figure 5A). HC serum showed no binding (eFigure 2, links.lww.com/NXI/A967).

The gephyrin signal serves as a postsynaptic marker and allows the quantification of GlyRβ (mEos) in gephyrin-positive clusters (Figure 5A). A comparison of gephyrin and GlyRβ between wild-type controls (*Glra1*$^{+/+}$/*Glrb*$^{eos/eos}$) and homozygous *oscillator* neurons (*Glra1*$^{spdot/spdot}$/*Glrb*$^{eos/eos}$) revealed significantly less GlyRβ in *oscillator* neurons ($^{**}p$ = 0.004), while gephyrin levels were indistinguishable between *oscillator* and wild-type controls (p = 0.35, Figure 5, B and C, eTable 1A (links.lww.com/NXI/A969). The reduced GlyRβ expression in *oscillator* neurons was not surprising because GlyRα1, the main partner of GlyRβ, is absent. Of interest, no significant differences were identified in the synaptic localization of GlyRβ between *Glra1*$^{spdot/spdot}$/*Glrb*$^{eos/eos}$ and *Glra1*$^{+/+}$/*Glrb*$^{eos/eos}$ neurons (p = 0.86, Figure 5D). The number of synapses targeted by Pat31 and Pat36 sera showed no differences between *Glra1*$^{+/+}$/*Glrb*$^{eos/eos}$ and *Glra1*$^{spdot/spdot}$/*Glrb*$^{eos/eos}$mice (p = 0.11 and p = 0.43, respectively, Figure 5E, eTable 1A).

Lack of GlyRα1 in homozygous *oscillator* mice was further validated using an α1-specific antibody (mAb2b) in Western blots of spinal cord, brainstem, and cortex tissue lysates (eFigure 3, A and B, links.lww.com/NXI/A968). Nevertheless, other GlyRα subunits (α2 and α3) were present in spinal cord (GlyR pan-α–positive protein samples, GlyRα2-positive staining of dissociated spinal cord neurons; eFigure 3A-B), and hence, binding of patient serum to other GlyRα subunits (α2 and α3) could be possible. However, cell-based analysis revealed no binding of Pat31 and Pat36 sera to GlyRα2 or α3 (eFigure 3C) confirming that binding of Pat31 and Pat36 aAbs is specific to GlyRβ.

At last, binding of Pat36 serum to GlyRβ was demonstrated by immunostaining of spinal cord sections of *Glra1*$^{spdot/spdot}$/*Glrb*$^{eos/eos}$ mice (Figure 5F). GlyRβ signals in *Glra1*$^{+/+}$/*Glrb*$^{eos/eos}$ spinal cord were stronger than in *Glra1*$^{spdot/spdot}$/*Glrb*$^{eos/eos}$. Similarly, serum staining was more intense to *Glra1*$^{+/+}$/*Glrb*$^{eos/eos}$ spinal cord while still present at *Glra1*$^{spdot/spdot}$/*Glrb*$^{eos/eos}$ dorsal and ventral horn spinal cord (Figure 5F, right images a_1, a_2, b_1, b_2). Our data clearly evaluated GlyRβ targeting of aAb from some patients suggesting GlyRβ as a new target for GlyR aAb in rare cases.

GlyR Ion Channel Function Is Altered Following Preincubation With GlyRβ-Positive Patient Sera

To investigate physiologic consequences of GlyRβ aAb targeting, ion channel function of GlyRs after preincubation with GlyRβ-positive patient serum was tested to assess whether similar molecular alterations exist as demonstrated for aAb against GlyRα.[5]

Whole-cell patch-clamp measurements of mixed spinal cord neurons from *Glra1*$^{spdot/spdot}$/*Glrb*$^{eos/eos}$ and *Glra1*$^{+/+}$/*Glrb*$^{eos/eos}$ mice demonstrated almost absent glycine-induced I_{max} for *Glra1*$^{spdot/spdot}$/*Glrb*$^{eos/eos}$ neurons lacking GlyRα1, while wild-type neurons showed large glycine-induced chloride currents (*Glra1*$^{+/+}$/*Glrb*$^{eos/eos}$: 2.1 ± 0.3 nA; *Glra1*$^{spdot/spdot}$/*Glrb*$^{eos/eos}$: 0.04 ± 0.01 nA, $^{****}p < 0.0001$) (Figure 6, A and B, eTable 1B, links.lww.com/NXI/A969). This excluded primary neurons from *Glra1*$^{spdot/spdot}$/*Glrb*$^{eos/eos}$ for investigation of the functional consequences of GlyRβ aAb. To better discriminate between the effects of aAbs

Figure 4 Preadsorption of Patient Sera With GlyRα1 Offers Specific Detection of aAbs to GlyRβ

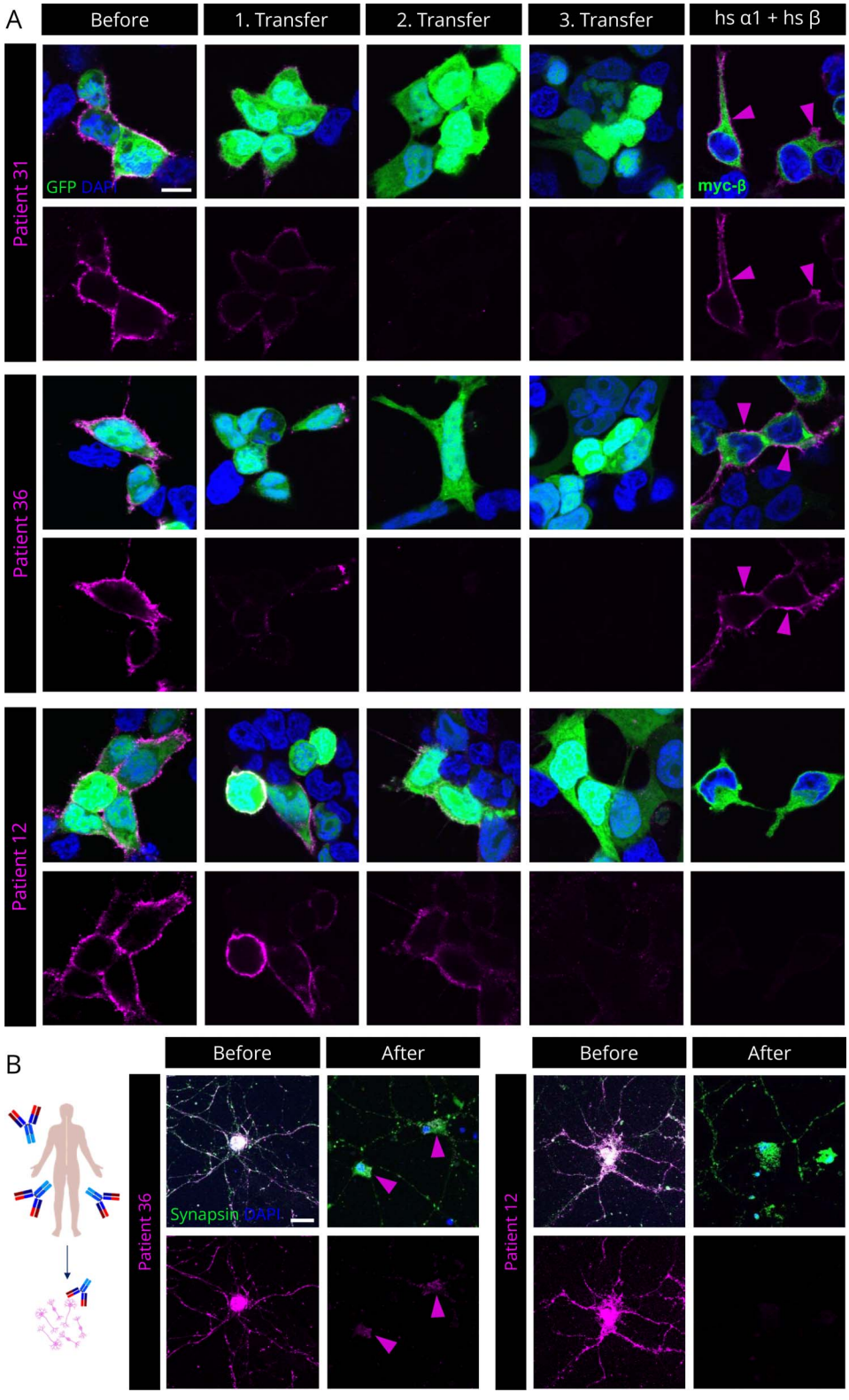

(A) Serum samples of Pat31, Pat36, and Pat12 were incubated on HEK-293 cells expressing the GlyRα1 subunit. After transfer of the supernatant for 3 times, cells cotransfected with zebrafish GlyRα1 and myc-tagged human GlyRβ were stained. GlyRβ is shown in green (right panel) and binding of patient serum in magenta. Arrows point to binding of patient serum to transfected HEK-293 cells after preadsorption. Note, while patient serum was added to living cells, the detection of the GlyRβ subunit through the myc antibody required cell fixation and permeabilization, leading to also intracellular staining of GlyRβ. Scale bar refers to 10 μm. (B) aAb binding to primary neurons (left). Mixed spinal cord neuronal cultures were stained (right images) with patient serum before and after preadsorption of Pat36 serum by ELISA plates coated with GlyRα1 ECD. Synapsin (green) is used as synapse marker and serum binding is shown in magenta. Scale bar refers to 20 μm.

against GlyRα1 and GlyRβ, we turned back and transfected HEK-293 cells with either human GlyRα1^{hs} subunit alone, or coexpressed zebrafish GlyRα1^{dr} with human GlyRβ. Similar to findings by Rauschenberger et al.,[5] patient serum binding to human GlyRα1 subunit led to a rightward shift in dose-response curves (untreated: 74 ± 4 μM; HC: 77 ± 6 μM; Pat31: 108 ± 12 μM, $p = 0.003$ compared with untreated and $p = 0.01$ compared with HC; Pat36: 100 ± 9 μM, $p = 0.01$

Figure 5 Patient Serum Binding to Neuronal GlyRβ Subunits Confirms GlyR Beta-Specific Binding

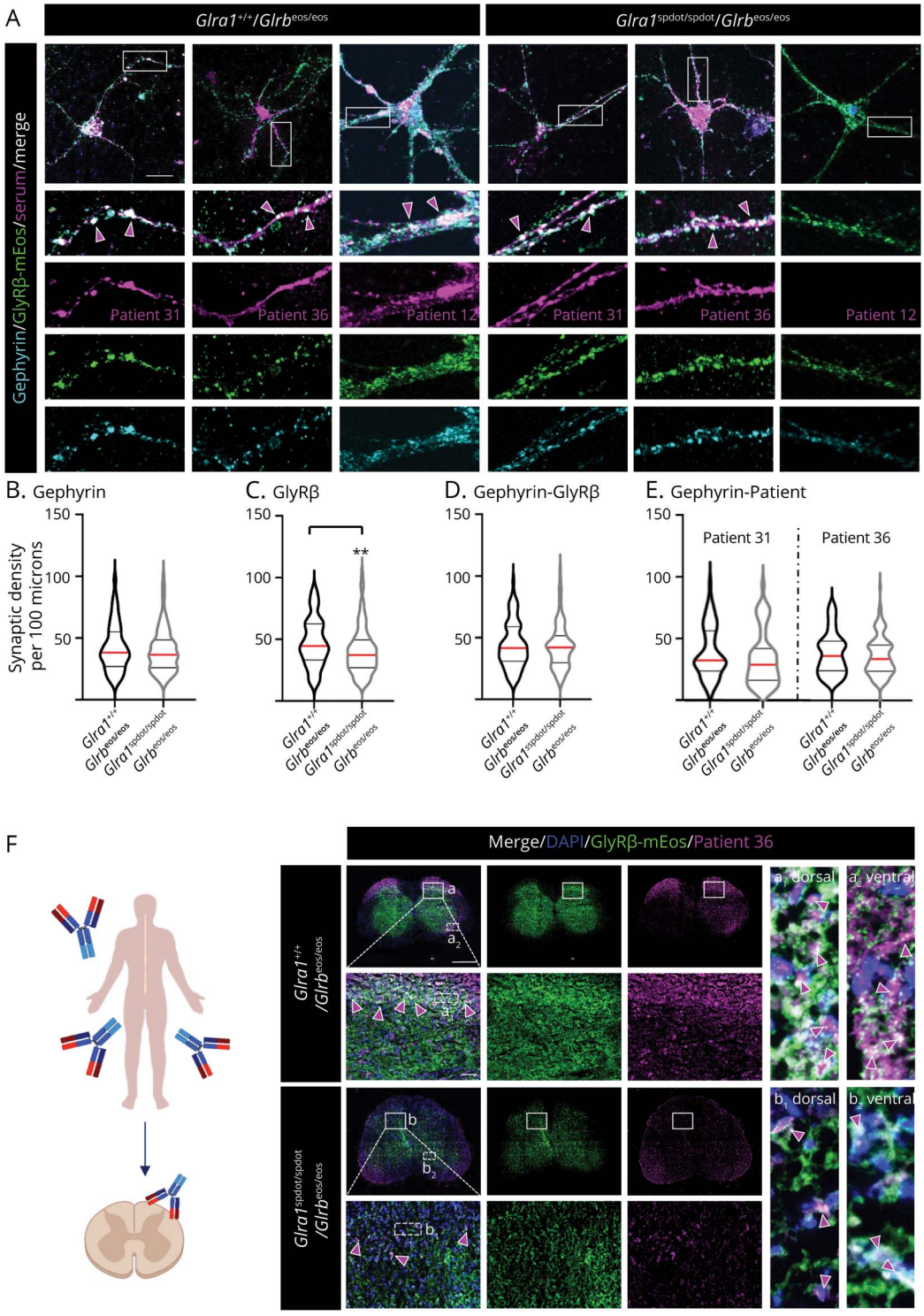

(A) Immunocytochemical stainings with serum samples of Pat31, Pat36, and another patient serum exclusively binding to GlyRα1 (Pat12) of mixed primary spinal cord neuronal cultures of *Glra1*$^{spdot/spdot}$/*Glrb*$^{eos/eos}$ and *Glra1*$^{+/+}$/*Glrb*$^{eos/eos}$ mice. *Glra1*$^{spdot/spdot}$/*Glrb*$^{eos/eos}$ and *Glra1*$^{+/+}$/*Glrb*$^{eos/eos}$ neurons were stained with antibodies against GlyRβ mEos (green), human-IgG (magenta), and gephyrin (cyan). Arrows point to colocalizing GlyRβ mEos and patient serum signals. Scale bars refer to 20 µm and 5 µm in magnification. (B–E) Quantification of synaptic density/100 microns in *Glra1*$^{spdot/spdot}$/*Glrb*$^{eos/eos}$ and *Glra1*$^{+/+}$/*Glrb*$^{eos/eos}$neurons (n = 3). Data are shown in violin blots with a red line marking the median and black lines marking the quartiles. Levels of significance: $^{**}p < 0.01$ (gephyrin: n.s. $p = 0.35$, n = 99 for *Glra1*$^{+/+}$/*Glrb*$^{eos/eos}$ and n = 123 for *Glra1*$^{spdot/spdot}$/*Glrb*$^{eos/eos}$; GlyRβ: $^{**}p = 0.004$, n = 98 and n = 120; gephyrin-GlyRβ: n.s. $p = 0.86$, n = 97 and n = 123; gephyrin-Pat31: n.s. $p = 0.11$, n = 70 and n = 56); gephyrin-Pat36: n.s. $p = 0.43$, n = 97 and n = 118). (F) Immunohistochemical stainings with Pat36 serum of *Glra1*$^{+/+}$/*Glrb*$^{eos/eos}$ and *Glra1*$^{spdot/spdot}$/*Glrb*$^{eos/eos}$ spinal cord slices with antibodies against GlyRβ mEos (green) and human IgG (magenta). Arrows point to binding of patient serum to spinal cord slices colocalizing with GlyRβ signal in the enlarged images (white rectangles in upper row; a and b). Scale bar refers to 500 µm and 50 µm in magnification. Further inlets (white dotted rectangles, a_1 dorsal, a_2 ventral, b_1 dorsal, b_2 ventral) are shown on the right with pink arrow heads pointing to colocalization between GlyRβ and patient serum.

Figure 6 Electrophysiologic Characterization of GlyR aAb Binding to the GlyRβ Subunit

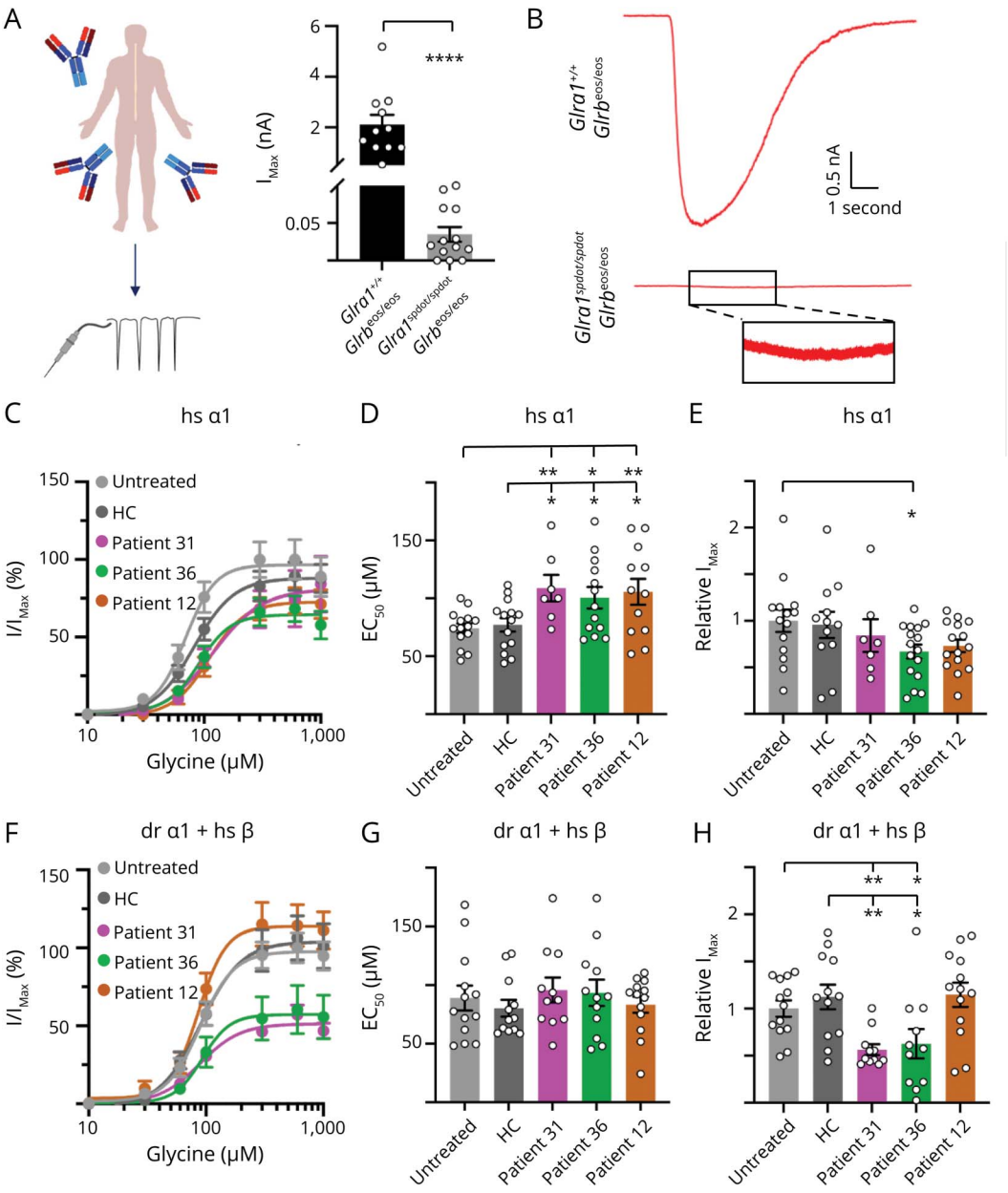

(A) Whole-cell patch-clamp measurements of glycine-induced maximal currents of *Glra1*$^{+/+}$/*Glrb*$^{eos/eos}$ and *Glra1*$^{spdot/spdot}$/*Glrb*$^{eos/eos}$ neurons. Data are shown in bar diagrams with mean ± SEM and individual data points (*Glra1*$^{+/+}$/*Glrb*$^{eos/eos}$: n = 11, *Glra1*$^{spdot/spdot}$/*Glrb*$^{eos/eos}$: n = 13, ****p < 0.0001). (B) Exemplary maximal currents induced by 1 mM glycine of *Glra1*$^{+/+}$/*Glrb*$^{eos/eos}$ and *Glra1*$^{spdot/spdot}$/*Glrb*$^{eos/eos}$ neurons. (C) Dose-response curves of HEK-293 cells transfected with hsGlyRα1 to increasing glycine concentrations (10, 30, 60, 100, 300, 600, 1,000 μM) either untreated or preincubated for 1 hour with Pat31, Pat36, Pat12, or healthy control (HC) serum. (D and E) Resulting EC_{50} values and maximal currents for HEK-293 cells transfected with human (hs) GlyRα1. Data are shown in bar diagrams with mean ± SEM and individual data points (untreated: n = 14, Pat31: n = 7, Pat36: n = 13, Pat12: n = 12, HC: n = 14). (F) Dose-response curves of HEK-293 cells transfected with zebrafish (dr) GlyRα1 and hs GlyRβ to increasing glycine concentrations (10, 30, 60, 100, 300, 600, 1,000 μM) either untreated or preincubated for 1 hour with Pat31, Pat36, Pat12, or HC serum. (G–H) Resulting EC_{50} values and maximal currents for HEK-293 cells transfected with zebrafish (dr) GlyRα1 and hs GlyRβ. Data are shown in bar diagrams with mean ± SEM and individual data points (untreated: n = 12, Pat31: n = 11, Pat36: n = 12, Pat12: n = 13, HC: n = 13). Levels of significance: *p < 0.05, **p < 0.01, ***p < 0.001, ****p < 0.0001.

compared with untreated and p = 0.04 compared with HC; Pat12: 106 ± 11 μM, p = 0.009 compared with untreated and p = 0.03 compared with HC) and thus a reduced receptor potency (Figure 6, C and D). Binding of Pat36 serum but not Pat12 and Pat31 sera resulted in a slightly decreased maximal current (relative I_{max} to untreated: 100 ± 12%; HC: 95 ± 14%; Pat31: 84 ± 18%; Pat36: 67 ± 7%, p = 0.02 compared with untreated Pat12: 73 ± 7%; Figure 6E, see also eTable 1C, links.lww.com/NXI/A969). By contrast, binding of patient serum to GlyRβ (zebrafish GlyRα1^{dr} with human GlyRβ were transfected) did significantly decrease maximal currents after preincubation with both Pat31 (56% ± 5.8%) and Pat36 (52% ± 14.6%) sera compared with untreated (100% ± 8.6%) and HC treated (105% ± 13.8%) cells (Pat 31: **p = 0.001 compared with untreated and **p = 0.002 compared with HC; Pat 36: *p = 0.02 compared with untreated and *p = 0.04

compared with HC; Figure 6, F–H, see also eTable 1C) arguing for less glycine efficacy.

In sum, while binding of patient aAb to GlyRα subunits leads to reduced glycine potency, binding to GlyRβ results in reduced maximal glycine-gated currents and hence reduced glycine efficacy. Therefore, GlyR aAbs targeting distinct GlyR subunits affect glycinergic function differently, thus arguing for a significant contribution of both GlyRα1-specific and GlyRβ-specific aAb to the disease pathology.

Discussion

GlyR aAbs are involved in the pathology of SPS and PERM. Binding of GlyR aAb mainly to GlyRα1 but also to other α subunits has been described.[4] Although the GlyRβ subunit shares a high homology to GlyRα subunits in its ECD, no detection of GlyRβ-specific aAb has been exhibited, yet. In this study, we found the GlyRβ subunit as a novel target for GlyR aAb in 2 human patients experiencing SPS/PERM or focal epilepsy. Specificity for GlyRβ was achieved using an N-terminal myc-tagged GlyRβ variant coexpressed with zebrafish GlyRα1 mainly not bound by patients with GlyRα1-specific aAb.[5,18] Among 58 patient sera investigated, 30 were positive for GlyRα1 binding, 2 patients in addition targeted GlyRβ specifically. Patient sera negative for GlyRα1 binding did also not respond to GlyRβ arguing most probably against an SPS/PERM phenotype with exclusively GlyRβ aAb.

We confirmed specific binding of patient-derived GlyRβ aAb at spinal cord neurons and tissue sections of a novel generated hybrid mouse line expressing an mEos-tagged GlyRβ but lacked GlyRα1 (*oscillator*).[14,37] The signal obtained by the patient serum with GlyRβ aAb colocalized with gephyrin, a direct interaction partner of GlyRβ at synaptic sites. A 1:1 ratio of GlyRβ to gephyrin at synapses has been demonstrated; however, the overall GlyRβ amount in the hybrid line lacking GlyRα1 is significantly lower.[14] Other GlyRα subunits (α2 or α3) are possibly able to compensate for lack of GlyRα1 at synaptic sites. Our patients with GlyRβ aAb did, however, not bind mouse GlyRα2 or α3, confirming the specificity of patient aAb to GlyR β in spinal cord tissue.

Patients experiencing SPS/PERM show similar symptoms to patients with startle disease. Startle disease is due to variants in genes affecting glycinergic inhibition (*GLRA1* encoding the GlyRα1 subunit, *SLC6A5* (GlyT2) and *GLRB* (GlyRβ)).[38] *GLRB* variants decrease synaptic localization of heteromeric GlyRs or impair receptor function.[16,18] Moreover, single-nucleotide variations in *GLRB* have been shown in humans with enhanced agoraphobic behavior.[34,35] Enhanced anxiety has also been reported for patients with startle disease being afraid for unexpected acoustic stimuli.[39,40] Our patients underwent questionnaires for anxiety, ASI, enhanced sensitivity to different stimuli, and pain. Patients with SPS exhibited a higher sensitivity score for noise, visual, somatosensory, and emotional excitement in line with typical SPS symptoms. The patient with focal epilepsy exhibited moderate to severe anxiety. Several reports exhibited mRNA and protein expression of GlyRα and β in thalamic and midbrain areas, brain regions involved in anxiety circuits.[14,41,42]

For GlyRα1, a common N-terminal epitope has been determined by a chimeric approach making use of nonbinding to the zebrafish GlyRα1 but to the human α1.[5] Although with limitations, another option to fine-map aAb binding sites is the use of peptide microarrays.[27,36] Depending on the protein region targeted by the aAb, discontinuous or continuous epitopes have to be evaluated. Discontinuous epitopes require chemical approaches and/or experimental mimicking or computer-based predictions and are used if highly ordered structures are targeted, while continuous epitopes are usually observed when autoantibodies bind to disordered regions. Using a continuous overlapping peptide library, distinct GlyRβ autoantibody binding sequences ^{77}GIPVDVVVNIFINSF^{91} and ^{141}PDLFFANEKSANFHDV^{156} were identified. The determined binding sequence in the patient with focal epilepsy overlaps only partially between GlyRα and GlyRβ. The second epitope ^{141}P-^{156}V identified in patients with SPS/PERM is localized close to and overlapping with the binding site of mAb4a, a widely used commercial antibody that binds all GlyRα subunits and to some extent GlyRβ. The observed pan reactivity is therefore mediated by an autoantibody that recognizes a conserved motif shared between subunits. The cell-based preadsorption experiment, however, indicates that there is an additional exclusive GlyRβ-specific epitope. Whether the effect on efficacy is mediated by aAb binding to the mapped epitope or an epitope that could not be resolved in the array-based mapping analysis requires further studies, e.g., chimeric approaches. Binding of GlyRα1-specific aAb from the same patient serum might also be enabled through other immunogenic regions as previously determined.[5]

Because it was recently shown that GlyRs assemble as 4α:1β, binding of an aAb against GlyRβ most likely leads to cross-linking of 2 receptors leading subsequently to receptor internalization.[8,9] Internalization of aAb-targeted GlyRs may thus underlie the observed reduced receptor efficacy. By contrast, functional alterations following aAb binding to exclusively the GlyRα subunit showed decreased receptor potency in line with previous observations and most probably due to conformational blocking.[5] In addition, Crisp et al.[6] demonstrated disrupted glycinergic neurotransmission in recordings from spinal cord neurons preincubated with patient sera and with Fab fragments suggesting that the functional impairment does not require cross-linking of receptors. Hence, our data provide evidence that patients harboring aAb against GlyRα1 and β experience pronounced impairment of glycinergic inhibition by affected glycine efficacy and potency.

In this study, we show that GlyR aAb not only target GlyRα subunits but also in some cases GlyRβ. With this novel contribution to the SPS/PERM disease pathology, we extend the

current knowledge of the molecular mechanism by substantially decreased inhibition at glycinergic synapses due to reduced glycine efficacy and potency. Whether the identified pathomechanism act in an additive manner or independent still needs to be verified. A detailed binding pattern investigation of similarities and differences in the aAb repertoire of patients will help to identify personalized aAb profiles and thus offer novel treatment options.

Acknowledgment

The authors thank Christine Schmitt and Dana Wegmann for excellent technical assistance. Dr. Christian Specht, INSERM U1195, Paris, France is highly acknowledged for providing the *Glrb*eos mouse line for this study.

Study Funding

This work was supported by Deutsche Forschungsgemeinschaft (DFG) SO328/9-1 (CS) and VI586/8-1, Research unit SYNABS FOR3004. A. Wiessler, I. Talucci, I. Piro, and S. Seefried are supported by the GSLS Wuerzburg, Germany. H.M. Maric and I. Talucci acknowledge funding by the Interdisziplinaeres Zentrum fuer Klinische Forschung (IZKF) of Wuerzburg, project number A-F-N-419 and DFG (MA6957/1-1).

Disclosure

The authors report no disclosures relevant to the manuscript. Go to Neurology.org/NN for full disclosures.

Publication History

Received by *Neurology: Neuroimmunology & Neuroinflammation* July 10, 2023. Accepted in final form October 2, 2023. Submitted and externally peer reviewed. The handling editor was Editor Josep O. Dalmau, MD, PhD, FAAN.

Appendix Authors

Name	Location	Contribution
Anna-Lena Wiessler, MSc	Institute for Clinical Neurobiology, University of Wuerzburg, Germany	Drafting/revision of the article for content, including medical writing for content; major role in the acquisition of data; and analysis or interpretation of data
Ivan Talucci, MSc	Department of Neurology, University Hospital Wuerzburg; Rudolf Virchow Center for Integrative and Translational Bioimaging, University of Wuerzburg, Germany	Major role in the acquisition of data; analysis or interpretation of data
Inken Piro, MSc	Department of Neurology, University Hospital Wuerzburg, Germany	Major role in the acquisition of data; analysis or interpretation of data
Sabine Seefried, MSc	Department of Neurology, University Hospital Wuerzburg, Germany	Analysis or interpretation of data
Verena Hörlin	Institute for Clinical Neurobiology, University of Wuerzburg, Germany	Major role in the acquisition of data; analysis or interpretation of data
Betül B. Baykan, MD	Department of Neurology, Istanbul Faculty of Medicine, Istanbul University, Turkey	Major role in the acquisition of data; analysis or interpretation of data
Erdem Tüzün, MD	Institute of Experimental Medical Research, Istanbul University, Turkey	Drafting/revision of the article for content, including medical writing for content; major role in the acquisition of data; study concept or design; and analysis or interpretation of data
Natascha Schaefer, Dr.	Institute for Clinical Neurobiology, University of Wuerzburg, Germany	Major role in the acquisition of data; analysis or interpretation of data
Hans M. Maric, Dr.	Rudolf Virchow Center for Integrative and Translational Bioimaging, University of Wuerzburg, Germany	Drafting/revision of the article for content, including medical writing for content; study concept or design; and analysis or interpretation of data
Claudia Sommer, MD	Department of Neurology, University Hospital Wuerzburg, Germany	Drafting/revision of the article for content, including medical writing for content; study concept or design; and analysis or interpretation of data
Carmen Villmann, Prof. Dr.	Institute for Clinical Neurobiology, University of Wuerzburg, Germany	Drafting/revision of the article for content, including medical writing for content; study concept or design

References

1. Hutchinson M, Waters P, McHugh J, et al. Progressive encephalomyelitis, rigidity, and myoclonus: a novel glycine receptor antibody. *Neurology*. 2008;71(16):1291-1292. doi:10.1212/01.wnl.0000327606.50322.f0
2. Balint B, Bhatia KP. Stiff person syndrome and other immune-mediated movement disorders - new insights. *Curr Opin Neurol*. 2016;29(4):496-506. doi:10.1097/WCO.0000000000000351
3. Henningsen P, Meinck HM. Specific phobia is a frequent non-motor feature in stiff man syndrome. *J Neurol Neurosurg Psychiatry*. 2003;74(4):462-465. doi:10.1136/jnnp.74.4.462
4. Carvajal-González A, Leite MI, Waters P, et al. Glycine receptor antibodies in PERM and related syndromes: characteristics, clinical features and outcomes. *Brain*. 2014;137(Pt 8):2178-2192. doi:10.1093/brain/awu142
5. Rauschenberger V, von Wardenburg N, Schaefer N, et al. Glycine receptor autoantibodies impair receptor function and induce motor dysfunction. *Ann Neurol*. 2020;88(3):544-561. doi:10.1002/ana.25832
6. Crisp SJ, Dixon CL, Jacobson L, et al. Glycine receptor autoantibodies disrupt inhibitory neurotransmission. *Brain*. 2019;142(11):3398-3410. doi:10.1093/brain/awz297
7. Du J, Lü W, Wu S, Cheng Y, Gouaux E. Glycine receptor mechanism elucidated by electron cryo-microscopy. *Nature*. 2015;526(7572):224-229. doi:10.1038/nature14853
8. Yu H, Bai XC, Wang W. Characterization of the subunit composition and structure of adult human glycine receptors. *Neuron*. 2021;109(17):2707-2716.e6. doi:10.1016/j.neuron.2021.08.019
9. Zhu H, Gouaux E. Architecture and assembly mechanism of native glycine receptors. *Nature*. 2021;599(7885):513-517. doi:10.1038/s41586-021-04022-z
10. Lynch JW. Molecular structure and function of the glycine receptor chloride channel. *Physiol Rev*. 2004;84(4):1051-1095. doi:10.1152/physrev.00042.2003
11. Lynch JW. Native glycine receptor subtypes and their physiological roles. *Neuropharmacology*. 2009;56(1):303-309. doi:10.1016/j.neuropharm.2008.07.034
12. Turecek R, Trussell LO. Presynaptic glycine receptors enhance transmitter release at a mammalian central synapse. *Nature*. 2001;411(6837):587-590. doi:10.1038/35079084
13. Kneussel M, Betz H. Receptors, gephyrin and gephyrin-associated proteins: novel insights into the assembly of inhibitory postsynaptic membrane specializations. *J Physiol*. 2000;525(Pt 1):1-9. doi:10.1111/j.1469-7793.2000.t01-4-00001.x
14. Maynard SA, Rostaing P, Schaefer N, et al. Identification of a stereotypic molecular arrangement of endogenous glycine receptors at spinal cord synapses. *Elife*. 2021;10:e74441. doi:10.7554/eLife.74441

15. Grudzinska J, Schemm R, Haeger S, et al. The beta subunit determines the ligand binding properties of synaptic glycine receptors. *Neuron*. 2005;45(5):727-739. doi:10.1016/j.neuron.2005.01.028
16. James VM, Bode A, Chung SK, et al. Novel missense mutations in the glycine receptor beta subunit gene (GLRB) in startle disease. *Neurobiol Dis.* 2013;52:137-149. doi:10.1016/j.nbd.2012.12.001
17. Kingsmore SF, Giros B, Suh D, Bieniarz M, Caron MG, Seldin MF. Glycine receptor beta-subunit gene mutation in spastic mouse associated with LINE-1 element insertion. *Nat Genet*. 1994;7(2):136-141. doi:10.1038/ng0694-136
18. Piro I, Eckes AL, Kasaragod VB, et al. Novel functional properties of missense mutations in the Glycine receptor beta subunit in startle disease. *Front Mol Neurosci*. 2021;14:745275. doi:10.3389/fnmol.2021.745275
19. Ekizoglu E, Baykan B, Sezgin M, et al. Follow-up of patients with epilepsy harboring antiglycine receptor antibodies. *Epilepsy Behav*. 2019;92:103-107. doi:10.1016/j.yebeh.2018.09.034
20. Dixon D, Pollard B, Johnston M. What does the chronic pain grade questionnaire measure? *Pain*. 2007;130(3):249-253. doi:10.1016/j.pain.2006.12.004
21. Von Korff M, Ormel J, Keefe FJ, Dworkin SF. Grading the severity of chronic pain. *Pain*. 1992;50(2):133-149. doi:10.1016/0304-3959(92)90154-4
22. Liebowitz MR. Social phobia. *Mod Probl Pharmacopsychiatry*. 1987;22:141-173. doi:10.1159/000414022
23. Soykan C, Ozgüven HD, Gençöz T. Liebowitz Social Anxiety Scale: the Turkish version. *Psychol Rep*. 2003;93(3 Pt 2):1059-1069. doi:10.2466/pr0.2003.93.3f.1059
24. Dalakas MC, Fujii M, Li M, McElroy B. The clinical spectrum of anti-GAD antibody-positive patients with stiff-person syndrome. *Neurology*. 2000;55(10):1531-1535. doi:10.1212/wnl.55.10.1531
25. Fischhaber N, Faber J, Bakirci E, et al. Spinal cord neuronal network formation in a 3D printed reinforced matrix-A model system to study disease mechanisms. *Adv Healthc Mater*. 2021;10(19):e2100830. doi:10.1002/adhm.202100830
26. Rauschenberger V, Piro I, Kasaragod VB, et al. Glycine receptor autoantibody binding to the extracellular domain is independent from receptor glycosylation. *Front Mol Neurosci*. 2023;16:1089101. doi:10.3389/fnmol.2023.1089101
27. Schulte C, Khayenko V, Maric HM. Peptide microarray-based protein interaction studies across affinity ranges: enzyme stalling, cross-linking, depletion, and neutralization. *Methods Mol Biol*. 2023;2578:143-159. doi:10.1007/978-1-0716-2732-7_10
28. Pribilla I, Takagi T, Langosch D, Bormann J, Betz H. The atypical M2 segment of the beta subunit confers picrotoxinin resistance to inhibitory glycine receptor channels. *Embo J*. 1992;11(12):4305-4311. doi:10.1002/j.1460-2075.1992.tb05529.x
29. Schindelin J, Arganda-Carreras I, Frise E, et al. Fiji: an open-source platform for biological-image analysis. *Nat Methods*. 2012;9(7):676-682. doi:10.1038/nmeth.2019
30. Bormann J, Rundström N, Betz H, Langosch D. Residues within transmembrane segment M2 determine chloride conductance of glycine receptor homo- and hetero-oligomers. *Embo J*. 1993;12(10):3729-3737. doi:10.1002/j.1460-2075.1993.tb06050.x
31. Doppler K, Schleyer B, Geis C, et al. Lockjaw in stiff-person syndrome with autoantibodies against glycine receptors. *Neurol Neuroimmunol Neuroinflamm*. 2016;3(1):e186. doi:10.1212/NXI.0000000000000186
32. Ekizoglu E, Tuzun E, Woodhall M, et al. Investigation of neuronal autoantibodies in two different focal epilepsy syndromes. *Epilepsia*. 2014;55(3):414-422. doi:10.1111/epi.12528
33. Sanli E, Akbayir E, Kuçukali CI, et al. Adaptive immunity cells are differentially distributed in the peripheral blood of glycine receptor antibody-positive patients with focal epilepsy of unknown cause. *Epilepsy Res*. 2021;170:106542. doi:10.1016/j.eplepsyres.2020.106542
34. Deckert J, Weber H, Villmann C, et al. GLRB allelic variation associated with agoraphobic cognitions, increased startle response and fear network activation: a potential neurogenetic pathway to panic disorder. *Mol Psychiatry*. 2017;22(10):1431-1439. doi:10.1038/mp.2017.2
35. Lueken U, Kuhn M, Yang Y, et al. Modulation of defensive reactivity by GLRB allelic variation: converging evidence from an intermediate phenotype approach. *Transl Psychiatry*. 2017;7(9):e1227. doi:10.1038/tp.2017.186
36. Talucci I, Maric HM. Peptide microarrays for studying autoantibodies in neurological disease. *Methods Mol Biol*. 2023;2578:17-25. doi:10.1007/978-1-0716-2732-7_2
37. Buckwalter MS, Cook SA, Davisson MT, White WF, Camper SA. A frameshift mutation in the mouse alpha 1 glycine receptor gene (Glra1) results in progressive neurological symptoms and juvenile death. *Hum Mol Genet*. 1994;3(11):2025-2030. doi:10.1093/hmg/3.11.2025
38. Chung SK, Bode A, Cushion TD, et al. GLRB is the third major gene of effect in hyperekplexia. *Hum Mol Genet*. 2013;22(5):927-940. doi:10.1093/hmg/dds498
39. Andermann F, Keene DL, Andermann E, Quesney LF. Startle disease or hyperekplexia: further delineation of the syndrome. *Brain*. 1980;103(4):985-997. doi:10.1093/brain/103.4.985
40. Kirstein L, Silfverskiold BP. A family with emotionally precipitated drop seizures. *Acta Psychiatr Neurol Scand*. 1958;33(4):471-476. doi:10.1111/j.1600-0447.1958.tb03533.x
41. Malosio ML, Marquèze-Pouey B, Kuhse J, Betz H. Widespread expression of glycine receptor subunit mRNAs in the adult and developing rat brain. *Embo J*. 1991;10(9):2401-2409. doi:10.1002/j.1460-2075.1991.tb07779.x
42. Waldvogel HJ, Baer K, Allen KL, Rees MI, Faull RL. Glycine receptors in the striatum, globus pallidus, and substantia nigra of the human brain: an immunohistochemical study. *J Comp Neurol*. 2007;502(6):1012-1029. doi:10.1002/cne.21349
43. Dalakas MC, Rakocevic G, Dambrosia JM, Alexopoulos H, McElroy B. A double-blind, placebo-controlled study of rituximab in patients with stiff person syndrome. *Ann Neurol*. 2017;82(2):271-277. doi:10.1002/ana.25002